Strojniški vestnik - Journal of Mechanical Engineering 70(2024)9-10, 452-465
DOI:10.5545/sv-jme.2023.897
Original Scientific Paper
Received for review: 2023-12-14
Received revised form: 2024-05-12
Accepted for publication: 2024-07-12

Lifespan Evaluation for a Standard RV Reducer based on Fatigue Strength Theory

Song Gao[1] – Yiwan Li[2] – Yueming Zhang[1,2] – Shuting Ji[1,2,*] – Jiapeng Wang[1]

[1] Beijing University of Technology, College of Mechanical & Energy Engineering, China
[2] Beijing Chietom-BJUT Intelligent Transmission Technology Research Institute Co., Ltd., China

Rotate vector (RV) reducers are the two-stage deceleration device comprising involute and cycloid-pin gear transmission mechanisms. As the typical deceleration elements, they are widely applied in industrial robots, digitally controlled machine tools and automation fields due to their compact structure and high precision. However, a reducer may lose precision after a long-term operation. Moreover, pitting and metal peeling of internal components may also occur, leading to a fatigue failure. Therefore, it is necessary to conduct investigations on lifespan evaluation for RV reducers. In this study, the CRV-80E reducer is taken as the research object. Firstly, according to its transmission characteristics, the lifespan evaluation model for a standard RV reducer is established based on fatigue strength theory and Palmgren-Miner linear cumulative damage law, with the internal crankshaft bearing is considered as the key component. Then, the simulations are carried out on crankshaft bearing by the ANSYS Workbench and SKF SimPro. The contact stress, deformation on bearing rollers, and the rated lifespan of the reducer are simulated. Finally, the accelerated life test is conducted on an RV reducer by increasing the external load with the positioning precision as an output and criterion. After the test, the reducer is disassembled, and metal peeling failure is observed on the crankshaft bearing while other parts are relatively intact. The test results validate the feasibility and accuracy of the service life evaluation model and simulation analysis. This study provides a new research approach for researchers and manufacturers and a design reference for engineers to improve the lifespan of RV reducers by optimizing crankshaft bearings, which have a certain academic value.

Keywords: RV reducer, lifespan evaluation, crankshaft bearing, simulation analysis, accelerated test

Highlights

- *The theoretical model of lifespan evaluation for RV reducer is established based on the fatigue strength theory.*
- *Simulation analysis is performed by ANSYS Workbench and SKF SimPro, obtaining the distributions of contact stress and deformation for bearing rollers, as well as the rated lifespan of the reducer.*
- *The accelerated life test of the RV reducer is processed with positioning precision as the evaluation criterion.*
- *Compared to other parts of the RV reducer, the crankshaft bearing is verified as the relatively weakest part.*

0 INTRODUCTION

Precision deceleration mechanisms applied to the joints for industrial robotic arms and automation fields are essential in mechanical manufacturing and aviation systems. As the typical deceleration device, rotate vector (RV) reducers are developed based on the cycloidal pinwheels and planetary gears transmission mechanism, and they are widely applied in industrial robots, rail transit, and wind power generation due to their compact structure, large transmission ratio, and high precision [1]. However, in applications, the transmission precision of RV reducer may be decreased due to fatigue aging. The reducer cannot operate when the decreased precision exceeds the allowable range, and the fatigue damage may also occur on the internal components. Furthermore, the rapid development exists in RV reducers in transmission principle, structure optimization and performance testing [2], while there is relatively little research on the service lifespan evaluation. Therefore, to better understand its working performance and reliability, it is necessary to develop feasible methods to evaluate the service lifespan of an RV reducer.

Numerous scholars have contributed to performance prediction for high-precision reducer, including inside components' geometric property analysis and structure design [3]. Hsieh and Aznar [4] developed the performance prediction method for cycloidal reducers. They analyzed the dynamic behavior of the RV reducer with varied design parameters such as pin roller number, roller pitch cycle radius, and cycloidal gear tooth number. The results indicated that transmission efficiency and stability were largely decreased with adopting more than two cycloidal gears in the reducer. Song et al. [5] analyzed the structure characteristics of the RV reducer, the contact stress and deformation for cycloid gear and crankshaft were simulated by finite element method (FEM). They illustrated that the crankshaft stiffness has a greater impact than cycloid gear on transmission precision. Blagojevic et al. [6] performed the contact stress analysis for cycloidal gear of a single-stage cycloid speed reducer, the specific solid model was

*Corr. Author's Address: Beijing University of Technology, College of Mechanical & Energy Engineering, 100 Pingleyuan, Chaoyang District, Beijing, China, jishuting@bjut.edu.cn

established by using FEM, and the experiment was carried out by strain gauges method for verification.

The RV reducer may experience fatigue failure in the working process, accompanied by decreased transmission precision and vibration. The study of failure mechanisms, fatigue life evaluation for reducers, and the analysis of weak components prone to damage have received the increasing attention. In application, it was verified that among the various components inside the RV reducer, generally, the crankshaft bearing is the weak component that first experiences fatigue damage in the mechanism. Therefore, it can be considered that the crankshaft bearing is the key component that determines the lifespan of the RV reducer. Zhao et al. [7] proposed an evaluation method for RV reducer based on a self-organizing feature map neural network algorithm. The fault identification model was established with the efficiency, square frequency, and power spectrum as selecting main parameters. The test examined evaluation results, showing that proposed model can determine the reducer's working performance. Zhi and Shang [8] introduced a remote monitoring method for fault diagnosis of RV reducer by collecting its feature extraction by information fusion. They verified that the diagnosis results could be applied to efficiency improvement and maintenance for reducers. Li et al. [9] modeled a 3D elastic-plastic contact model for RV reducer crankshaft, considering the hardness gradient and residual stress. They refined the fatigue criterion to enhance prediction, acknowledging the significant impact of initial stress on fatigue. Shot peening optimization improved fatigue performance and guided the anti-fatigue crankshaft design. Gao et al. [10] optimized the cycloid-pin gear mechanism for RV reducers based on enhancing the load-bearing capacity. The authors developed optimization models by researching influencing factors and optimized parameters using a genetic algorithm and verified through ANSYS simulation. Zhao et al. [11] proposed a multi-objective optimization method for cycloid-pin gears, which improved RV reducer's positioning accuracy and load-carrying capacity by considering backlash, transmission error, and torsional stiffness, largely improving transmission performance. The crankshaft bearing has the properties of a compacted structure and high operating speed, which is the key component for RV reducer. Huang et al. [12] applied the optimization design for the crankshaft bearing of the reducer by the crow search algorithm while considering the bearing geometry and the crowned profile of inside pin rollers. The bearing strength, reducer structure, and lubrication were considered constraints. After optimization, the lifespan of the crankshaft bearing presented effectively increased for two types of standard RV reducers.

An accelerated life test is a testing method for a lifespan that shortens the testing period by increasing external stress. The method was developed based on fatigue strength theory for researching component life [13]. Lee et al. [14] developed the accelerated life testing of powertrain components under cyclic loads for tractor transmission based on the Weibull-Inverse Power law, with the cumulative fatigue damage theory applied in the mechanism for diminishing the testing period and achieving the acceleration condition. The life testing period of the tractor system was largely reduced by increasing external load. Wang et al. [15] performed the efficiency testing of a special type reducer for automotive traction with a high fixed-ratio traction reducer as an object, and the efficiency map for transmission was established based on experimental results. They presented that the speed torque regions have the greatest effect on overall efficiency. Wang et al. [16] modeled cycloidal-pin gear meshing based on cycloidal reducer's multi-tooth characteristics. They analyzed system's meshing parameters and also determined contact area and dynamic wear coefficient via the simulation and regression, revealing pin-tooth patterns. Pin tooth wear significantly impacts meshing accuracy, affecting reducer precision and lifespan. Yang et al. [17] optimized geometric parameters of RV reducer with different target reliability as objectives based on the modified advanced mean value method. The results showed that the volume of the reducer was reduced while also meeting various reliability requirements by optimization, which provided a certain engineering value in the design and manufacture process for the RV reducer.

In this paper, taking the CRV-80E reducer as an object, based on fatigue strength theory, the theoretical model for lifespan evaluation of RV reducer under the variable load conditions is established. The effects of crankshaft bearing forces on the service life of the reducer were analyzed systematically, and the corresponding equations for estimating the rated life and service life of the reducer were derived. Next, the finite element simulation analysis was conducted on the crankshaft bearing to solve the contact stress and deformation for inside rollers through ANSYS Workbench and SKF SimPro, respectively, compared with theoretical results from proposed model. Then, the accelerated life test of the RV reducer was operated by simulating the actual working conditions at the robotic joint in practice. The loading method, rotating speed, and torque for each test stage were determined

based on S-curve acceleration and deceleration control algorithm. The experimental results were compared to both the theoretical model and simulation solution. The accelerated test reduced the period for verifying the service life of the reducer, but also diminished the time cost of durability testing. This research applied the fatigue strength theory to the reducer's crankshaft bearing and estimated the lifespan of RV reducers by calculating the service life of the crankshaft bearing. A relatively complete research system has been established by combining the theoretical model, simulation analyses, and experimental verification.

1 THEORETICAL MODEL

1.1 Transmission principle and fatigue life model

RV reducer is a new transmission type of high-precision planetary mechanism with the characteristics of two-stage deceleration and a large deceleration ratio comprising involute gears and cycloid-pin gears. Fig. 1 shows schematic diagram of the RV reducer's transmission principle and internal parts [18] and [19]. The first stage of deceleration is the involute gears mechanism, as the power is transmitted from the input shaft with gear ratio, the involute gears are meshed with the crankshaft by splines at the identical rotating speed. The second stage is the cycloid-pin gear drive mechanism with the crankshafts as the input components. The crankshafts and cycloidal gears are assembled through the crankshaft bearings. Due to the constraint of pin rollers uniformly arranged inside pin teeth shell, the cycloidal gear moves for one tooth by self-rotation in the opposite direction as it revolves for one circle. Finally, the self-rotation of cycloidal gears is transmitted to the support frame through crankshafts to achieve the two-stage deceleration. The support frame mesh with crankshaft and pin teeth shell by the tapered roller bearings and angular contact ball bearings, respectively.

As the basis for lifespan evaluation of mechanical components, fatigue strength theory depicts that the applied load for each time may cause variable damage to parts. The damage degree depends on the stress magnitude, as the larger stress corresponds to the greater damage, and it can be regarded as zero damage under low-stress levels. The main components of an RV reducer include the involute gear, crankshaft, cycloidal gear, pin roller, and bearing, and all are under variable stress during operation. When the reducer is subjected to torques from the external load, the inside components are constrained by various stresses as well [2] and [20], as shown in Eq. (1). Wherein, σ, T and F are stress, torque, and force that component is subjected to, respectively, i and j are the fatigue stress levels and N is cycle index of stress.

$$\left.\begin{aligned} \sigma_i^m \cdot N_i &= \sigma_j^m \cdot N_j \\ T_i^{m'} \cdot N_i &= T_j^{m'} \cdot N_j \\ F_i^{m'} \cdot N_i &= F_j^{m'} \cdot N_j \end{aligned}\right\}. \tag{1}$$

The stress on the internal parts of the RV reducer is under periodic variations when the multi-stage load is applied. The corresponding fatigue lifespan is evaluated using the cumulative fatigue strength theory [12], [21], and [22]. The Palmgren-Miner linear cumulative damage law also has widespread application [23]. Under the conditions of variable load loading, the magnitude of stress is $\sigma_1, \sigma_2, \ldots, \sigma_l$. Fatigue life corresponding to various amplitudes is $N_1, N_2, \ldots, N_l$, with the cycle numbers of $n_1, n_2, \ldots, n_l$. Thus, the lifespan damage under various stress amplitudes is n_i/N_i. Therefore, the cumulative damage amount at all stress levels can be expressed as

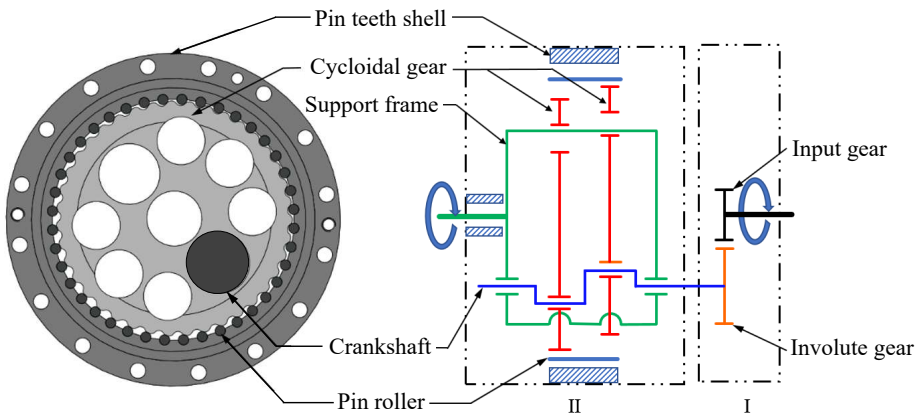

Fig. 1. *Transmission principle of RV reducer and inner components*

$\sum_{i=1}^{l}(n_i / N_i)$. Once a certain stress $\sigma_l (1 \le k \le l)$ is selected, the corresponding fatigue lifespan N_k with the constraints of stress and cycle number M_i can be calculated based on the Palmgren-Miner linear cumulative damage law through Eq. (2) [24].

$$N_k = \sum_{1}^{l} M_i \left(\frac{N_k}{N_i} \right). \tag{2}$$

The basic lifespan model of the RV reducer is derived by combining Eqs. (1) and (2), as shown in Eq. (3), which can be applied to each component that bears variable loads in the reducer. Wherein, F_i and T_i are the force and torque under graded load, respectively.

$$\left.\begin{aligned} N_k &= \sum_{1}^{l} M_i \left(\frac{F_i}{F_k} \right)^{m'} \\ N_k &= \sum_{1}^{l} M_i \left(\frac{T_i}{T_k} \right)^{m'} \end{aligned}\right\}. \tag{3}$$

The lifespan of the entire RV reducer is affected by the fatigue failure of core transmission parts such as involute gear, cycloid-pin gear, and different kinds of inside bearings. Due to the characteristics of small radial size and narrow crankshaft bearing structure, it is usually subjected to large fatigue stress with high-speed rotating. Generally, the crankshaft bearing is the first part to experience fatigue failure in application [25]. Therefore, it is reasonable to estimate that the crankshaft bearing determines the lifespan of the RV reducer. Furthermore, the lifespan of the crankshaft bearing is related to equivalent radial load, basic rated dynamic load, and output speed.

1.2 Lifespan Evaluation Model

1.2.1 Rated Service Life

During the transmission process, the crankshaft bearing contacts the cycloidal gear and crankshaft, and the stress analysis diagram is shown in Fig. 2a [24] and [26]. The pin gear is fixed, while the cycloidal gear rotated on a fixed axis subjected to the meshing force from the pin gear, and the small deformation Δu was generated on gear teeth. The joint force of the pin gear to the cycloidal gear is acted on point P, $O_{ci} (i = 1, 2, 3)$ is the center of the crankshaft, the coordinate $\sigma_{ci} (O_{ci} : x_i, y_i)$ are rigidly connected with the crankshafts, and θ is the included angle between x_1-axis and y-axis.

The force of the pin gear on the cycloidal gear can be decomposed into ΣP_{ix} and ΣP_{iy}, as shown in Eq. (4). Wherein, e is eccentricity, R_p is pin gear radius, Z_c and Z_p are tooth number of cycloidal and pin gear, respectively. Parameter k is the short amplitude coefficient, and $k = eZ_p / R_p$.

$$\left.\begin{aligned} \sum P_{ix} &= \frac{T}{2eZ_c} \\ \sum P_{iy} &= k_y \sum P_{ix} \end{aligned}\right\}, \tag{4}$$

$$k_y = \frac{2}{\pi} \left[\frac{1}{k} + \left(\frac{k^2 - 1}{2k^2} \right) \ln \frac{1+k}{1-k} \right]. \tag{5}$$

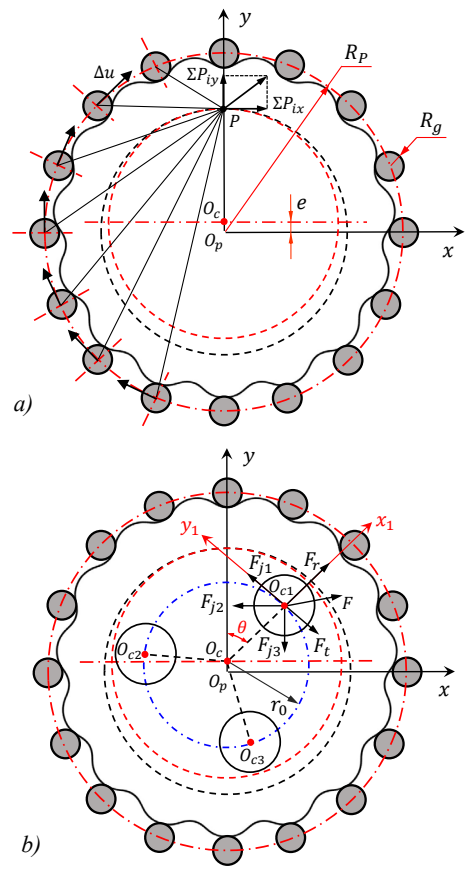

Fig. 2. *Schematic diagram of force analysis for cycloid gear of RV reducer; a) force between cycloid gear and pin roller, and b) force between cycloid gear and crankshaft bearing*

The assembly clearances between the cycloidal gear, crankshaft bearing, and pin gear are regarded as zero, and the friction is ignored here. Under the action of torque T, the component force of the crankshaft is equal in the tangential direction of $O_c O_{ci}$, which is $1/n$ of composition force, where n is the number of crankshafts. The cycloidal gear also bears force

F_j from the crankshaft bearing, as shown in Fig. 2b. F_j is decomposed to F_{j1}, F_{j2}, F_{j3}, here, F_{j2} and F_{j3} are realized force equilibrium with ΣP_{ix} and $\Sigma P_{i\ddot{y}}$, as given below. Parameter r_0 is the distribution circle radius for crankshafts.

$$\left.\begin{aligned} F_{j1} &= \frac{1}{N}\Sigma P_{ix}\frac{eZ_c}{r_0} \\ F_{j2} &= \frac{1}{N}\Sigma P_{ix} \\ F_{j3} &= \frac{k_y}{N}\Sigma P_{iy} \end{aligned}\right\}. \tag{6}$$

As shown in Fig. 2b, the force F on the crankshaft bearing can be decomposed into two parts of F_r and F_t along the radial and tangential direction in $O_{c1}(x_1, y_1)$, respectively. Based on copoint force balance [12], the equation is derived as follows:

$$\left.\begin{aligned} F_t &= F_{j1} + F_{j2}\cos\theta - F_{j3}\sin\theta \\ F_r &= F_{j2}\sin\theta + F_{j3}\cos\theta \end{aligned}\right\}. \tag{7}$$

The composition force of the crankshaft acting on the crankshaft bearing is given.

$$F = \sqrt{F_t^2 + F_r^2}. \tag{8}$$

The equivalent load for crankshaft bearing can be calculated by the following equations:

$$F_m = \left(\frac{\int_0^{2\pi} F^4 d\theta}{2\pi}\right)^{1/4} = KT_0, \tag{9}$$

$$K = \frac{1}{2NeZ_c r_0}\left[\begin{aligned} &4\left(1+k_y^2\right)\left(eZ_c\right)^2 r_0^2 + \\ &\left(1+k_y^2\right)^2 r_0^4 + \left(eZ_c\right)^4 \end{aligned}\right]^{1/4}. \tag{10}$$

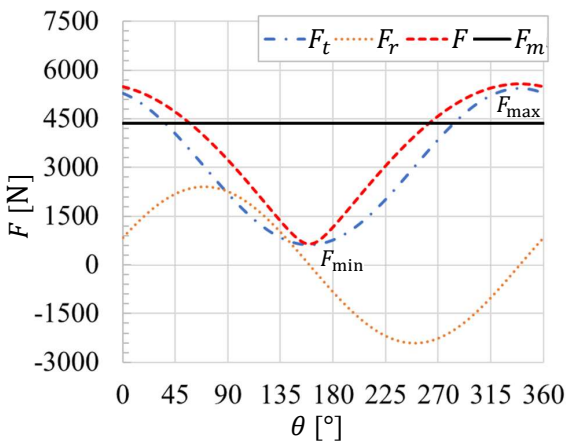

Fig. 3. *Force variations of crankshaft bearing within one transmission period*

In this study, the CRV-80E reducer is taken as an object. It is the standard RV reducer and the reducer is manufactured and provided by the Beijing Chietom-BJUT Intelligent Transmission Technology Research Institute Co., Ltd, wherein, C is the abbreviation of company name, 80E is the reducer's type. The basic structure parameters are as follows: e=1.45 mm, R_p=76.5 mm, Z_p=40, r_0=42 mm, T_0=784 N·m, and $Z_c = Z_i - 1$, and N=3. The force variation on the crankshaft bearing of the reducer within one period was obtained based on Eqs. (7) to (10), as shown in Fig. 3. It can be seen that the maximum load and equivalent dynamic load are undervalue of F_{max}=5576.2 N, F_m=4374.1 N, respectively.

The rated dynamic load of the crankshaft bearing represents bearing capacity of mechanism, which significantly affects the bearing life. The structural parameters for crankshaft bearing of the CRV-80E reducer are depicted in Fig. 4; the rated dynamic load for a single-row cylindrical roller bearing can be obtained by Eqs. (11) to (13) [27].

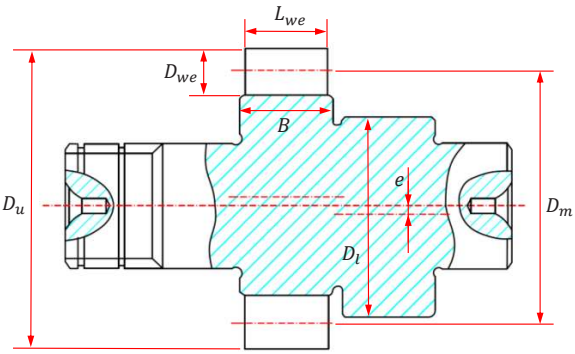

Fig. 4. *Schematic diagram of crankshaft bearing*

$$C_d = b_m f_c L_{we}^{7/9} Z^{3/4} D_{we}^{29/27}, \tag{11}$$

$$f_c = 208\lambda_v \gamma^{2/9}\left[\frac{(1-\gamma)^{29/27}}{(1+\gamma)^{1/4}}\right] \cdot \left\{1+\left[1.04\left(\frac{1-\gamma}{1+\gamma}\right)^{143/108}\right]^{9/2}\right\}^{-2/9}, \tag{12}$$

$$\gamma = \frac{D_{we}}{D_m}. \tag{13}$$

wherein, b_m and λ_v and are the correction factors of geometric precision and edge stress, respectively, and for radial roller bearing, they are taken as b_m=1.1 and λ_v=0.83 [27]. The other structural parameters of the crankshaft bearing are as follows: D_{we}=5 mm,

L_{we}=9 mm, Z=14, D_m=31 mm, r_0=47.5 mm. After calculation, the rated dynamic load of the crankshaft bearing is in value of C_d=21948.7 N.

In actual applications, the bearing rotating speed has a minor effect on the load. However, it has a great impact on fatigue life. The rated torque T_0 is defined as output torque under transmission efficiency η=75 %, and the rated life L_0 for RV reducer is represented by the lifespan of crankshaft bearing, as derived in Eq. (14). Parameter n_{out} is the revolution speed of the cycloidal gear, which is the mechanism's speed after being decelerated by the involute gear drive of the reducer. For the reducer, the rated output speed of n=15 rpm, and the cycloidal tooth number Z_c=39. The input revolution speed for cycloid-pin gear mechanism is obtained as $n \times Z_c$=585 rpm. Besides, it is necessary to consider the self-rotation of cycloid gear. When the cycloid gear rotates one circle, it also proceeds self-rotation by one tooth in reverse direction. Thus, the revolution speed of crankshaft bearing can be calculated as $n_{out}=n \times Z_c+n$=600 rpm. After calculation, the rated life of the CRV-80E reducer was obtained as L_0=6008 h. Parameter Z_p is pin roller number.

$$L_0 = \frac{10^6}{60 Z_p n_{out}} \left(\frac{C_d}{F_m} \right)^{10/3}. \tag{14}$$

Parameter F_0 is the load of crank bearing under rated torque T_0 and rated rotating speed n_0, F_a is the load under accelerated torque T_a and accelerated rotating speed n_a. The accelerated life L_a is defined. In mechanical transmission, the torque is proportional to the load. The accelerated coefficient A is cited in Eq. (15).

$$A = \frac{n_0}{n_a} \left(\frac{F_0}{F_a} \right)^{10/3} = \frac{n_0}{n_a} \left(\frac{T_0}{T_a} \right)^{10/3}. \tag{15}$$

1.2.2 Service Lifespan

RV reducers may encounter frequent starts and brakes, emergency stops, instantaneous heavy loads, and variable rotating speed in the actual working conditions. Thus, it is also necessary to explore the service life of reducers under operating conditions with variable speed and torque. Based on Eq. (3), set N_k is the fatigue life N_0 for the rated torque T_0, the Eq. (16) can be derived.

$$N_0 = \sum_1^l M_i \left(\frac{T_i}{T_0} \right)^{m'}. \tag{16}$$

There are various rotating speeds and torque during the start and break process. Here, the equivalent torque T_m is adopted for evaluating n_i and T_i for each period t_i.

$$T_m = \left[\frac{\sum (t_i n_i) T_i^{10/3}}{\sum t_i n_i} \right]^{3/10}. \tag{17}$$

The relationship between service life and rated life of RV reducers can be derived as follows:

$$L = \frac{L_0 n_0 T_0^{10/3}}{\sum t_i n_i T_i^{10/3} / \sum t_i} = \frac{L_0 n_0 T_0^{10/3}}{n_m T_m^{10/3}}. \tag{18}$$

where n_m is the equivalent rotating speed. The equation of service lifespan for reducer is obtained based on Eqs. (10), (14), and (18) are given below.

$$L = \frac{10^6 C_d^{10/3}}{60 Z_p n_m (K T_m)^{10/3}}. \tag{19}$$

The above equation depicts that when T_m or n_m is increased, i.e., increasing the external load or speed, the service life L can be diminished, which is the theoretical basis for the accelerated life test in Section 3.

2 SIMULATION ANALYSIS

2.1 Contact Stress and Deformation

According to Section 1.1, the lifespan of the RV reducer is mainly affected by crankshaft bearing. Therefore, the strength of the crankshaft bearing is the key to determining the service lifespan of the reducer. The contact strength of the crankshaft bearing can be analyzed based on Hertz's contact theory [28], which states that the contact type belongs to line contact. The stress is distributed as a semi-elliptical cylinder in the contact area for general bearings. The stress within the contact area can be calculated as defined in the following equations, where Q is the moment inertia of external load, is the contact half-width:

$$\sigma = \frac{2Q}{\pi L_{we} b}, \tag{20}$$

$$Q = \frac{4.6 F_r}{Z}, \tag{21}$$

$$b = 3.35 \times 10^{-3} \sqrt{\frac{Q}{L_{we} \sum \rho}}. \tag{22}$$

When a radial load is applied to the crankshaft bearing, only the lower half of the roller loading bearing is used. Due to the elastic deformation

between the rollers, the cycloidal gear, and the crankshaft, the inner ring of the bearing undergoes elastic deformation relative to the cycloidal gear, which can be calculated by Eq. (23) [27]. Parameters μ and E are the Poisson's ratio and elastic modulus, respectively. The pin rollers inside the bearing were selected as GCr15 steel with μ=0.3 and E=2.06×10^{11} N/mm^2.

$$\delta = \frac{2Q\left(1-\mu^2\right)}{\pi E L_{we}} \ln\left[\frac{\pi E L_{we}{}^2}{Q\left(1-\mu^2\right)\left(1 \mp \frac{D_{we}}{2}\right)}\right]. \quad (23)$$

Figs. 5 and 6 depict the contact stress and deformation of the crankshaft bearing for one period, respectively. The results show the maximum stresses were 1763.5 MPa and 1723.6 MPa for the inner and outer rings; for contact deformation, the maximum value showed 0.01012 mm and 0.01001 mm for the inner and outer rings, respectively. Parameter θ is the rotation angle of the crankshaft bearing, which corresponds to Fig. 2b. Moreover, both maximum values occurred at θ=340°.

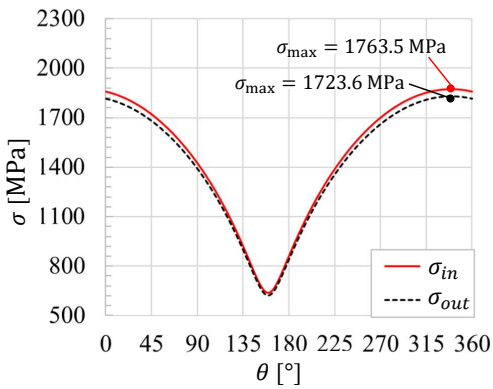

Fig. 5. *Variations of contact stress for inner and outer rings of crankshaft bearing within a single period*

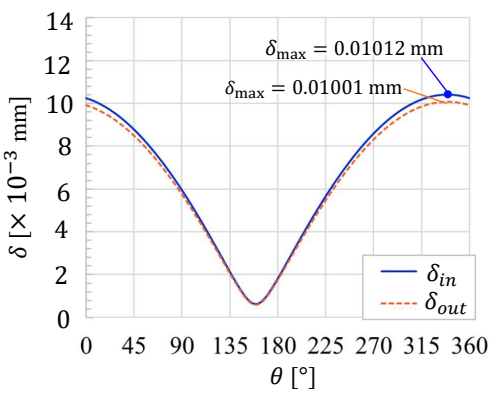

Fig. 6. *Variations of deformation for inner and outer rings of crankshaft bearing within a single period*

2.2 Ansys Finite Element Simulation

2.2.1 Grid Division

According to bearing structure parameters in Section 1.2.1, the finite element simulation of strength and stiffness for crankshaft bearing with one rotating period was carried out by ANSYS Workbench. Here, the crankshaft bearing was simplified to a component that only included three parts to ensure the simulation results' efficiency. The cycloidal gear, rollers, and crankshaft were selected as 20CrMo, GCr15, and 18CrNiMnMoA, respectively. The inner ring and rollers' thickness were set as 9 mm. Fixed support was applied on the outer ring, and tangential displacement was exerted on the eccentric part to prevent rollers from rotating around the center.

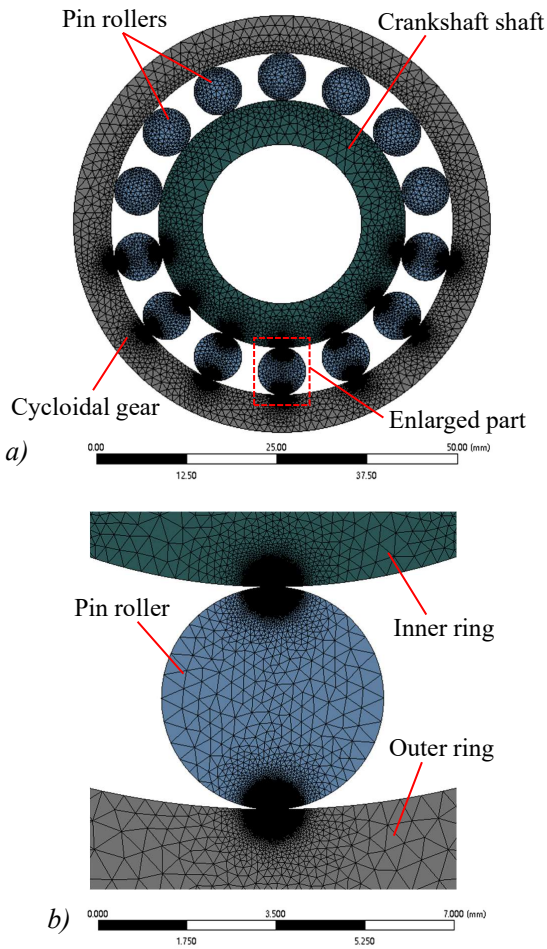

Fig. 7. *Grid division for crankshaft bearing; a) overview of grids, and b) enlarged part*

The simulation model was divided by the global triangles method with a size of 2 mm for grid elements,

the radius of 0.6 mm adopted the sphere local grids with an element size of 0.01 mm at vertexes between rollers and both rings. The overview and enlarged part of the grid division for crankshaft bearing are shown in Fig. 7.

2.2.2 Contact Stress

Fig. 8 shows the simulation solutions for the contact stress distribution of crankshaft bearing, applying an external load of 5576 N. It depicts that rollers at various positions correspond to various stress value presented by colors. The maximum contact stress occurred at the contact point between the inner ring and the lowest roller with the value of 1692.4 MPa, showing a 4.03 % error compared with the theoretical result. Moreover, the stress decreases as it approaches the bearing's upper part and outer ring.

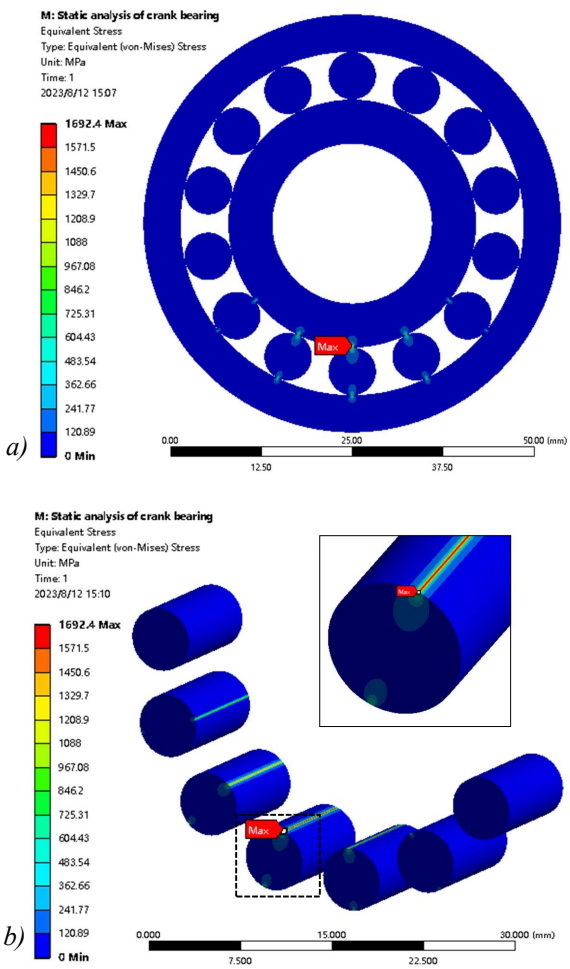

Fig. 8. *Simulation solutions of crankshaft bearing by ANSYS Workbench; a) overview of contact stress, and b) contact stress distribution of bearing rollers*

2.2.3 Contact Deformation

Fig. 9 shows the contact deformation distribution of the crankshaft bearing; the value varies for each pin roller inside the bearing. The maximum contact deformation is 0.010203 mm, at the same position with maximum stress, and there was a 0.82 % error compared with the theoretical result of 0.01012 mm. The accuracy of finite element simulation is related to the structure parameter precision of the crankshaft bearing and the adopted grid type in the analysis model.

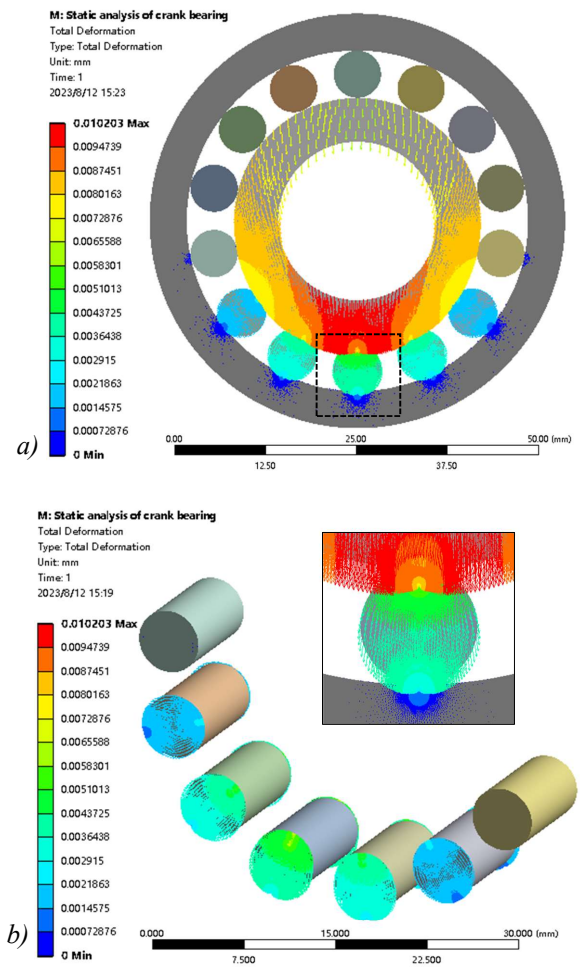

Fig. 9. *Simulation solutions of crankshaft bearing by ANSYS Workbench; a) overview of contact deformation, and b) deformation distribution of rollers*

2.3 SKF SimPro Service Lifespan Simulation

SKF SimPro analyzed the simulation of the service life of the RV reducer. The crankshaft bearing is selected as the analysis object in the simulation

process. Then the corresponding parameters are set for boundary, lubricating, and bearing gap to complete the model's establishment. The simulation solutions of contact stress and deformation for each roller inside the bearing are obtained, as shown in Fig. 10.

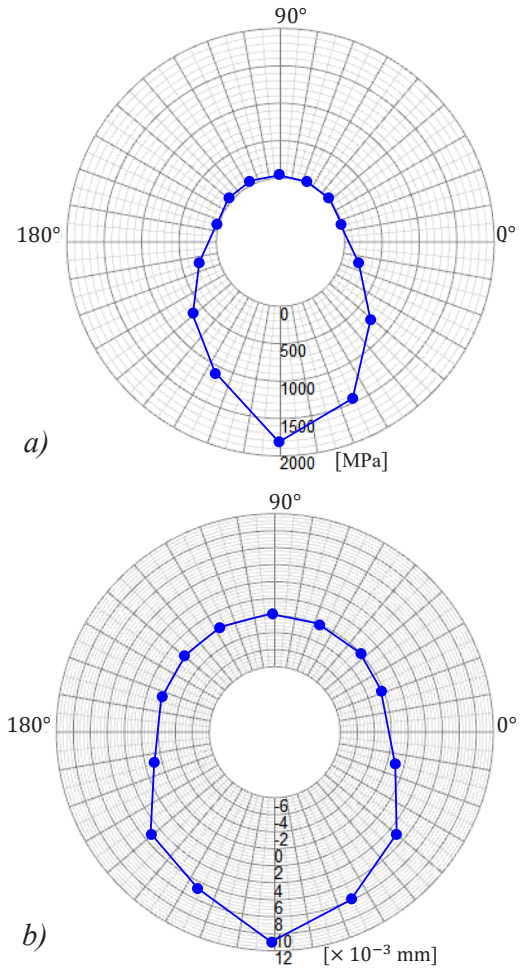

Fig. 10. *Simulation solutions of crankshaft bearing by SKF SimPro; a) contact stress, and b) deformation*

Due to the inability of Ansys to simulate bearing lifespan, SKF SimPro provides relatively rough simulation results for contact stress deformation for each roller of bearing. Therefore, this section combined the advantages of Ansys and SKF SimPro. Fig. 11 compares the simulation solutions for contact stress and deformation by ANSYS Workbench and SKF SimPro. Fig. 11 illustrates the distribution trends for the both parameters simulated from two softwares showed identical errors of 5.2 % and 6.9 %, respectively, i.e., they showed high correlations. The finite element simulation verified the theoretical results of the contact stress and contact deformation for bearing roller, which can indirectly verify the correctness of the theoretical model.

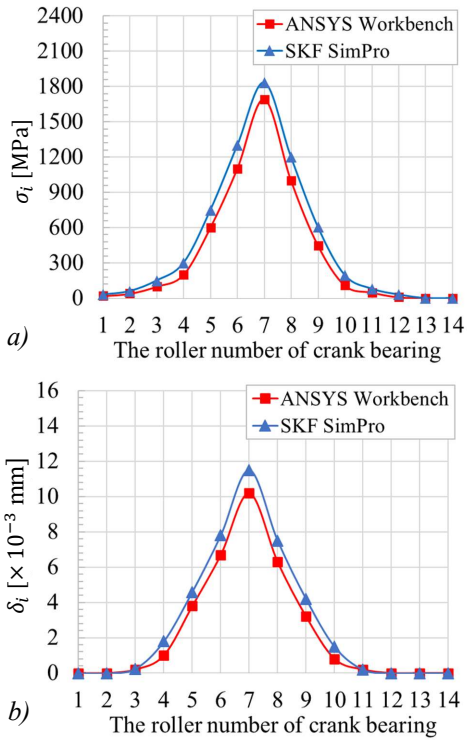

Fig. 11. *Simulation solutions of crankshaft bearing by SKF SimPro; a) contact stress, and b) deformation*

The simulation result for service life through SKF SimPro is as follows: the basic rated life for CRV-80E reducer (ISO 281, L_{10}h) is 6400 hours; the modified rated life is 7400 hours. The modified rated life is obtained with considering the conditions such as appropriate bearing clearance, sealing, and lubrication factors in simulation. Here, the basic rated life is regarded as the simulation result for fatigue lifespan of the reducer, i.e., 6400 hours. The results show that the error between simulation and theoretical model (Eq. (19)) is 6.52 %, which is within the allowable range. The comparisons verified the feasible and accuracy of theoretical model and simulations for RV reducer service lifespan evaluation.

3 ACCELERATED LIFE TEST

3.1 Testing Apparatus

In practice, RV reducers are generally applied in complicated conditions with frequent and reciprocating starts and breaks. The inside crankshaft bearings are prone to fatigue failure under inertia and impact. Therefore, when operating the service

life test on an RV reducer, it is advisable to simulate their working state. Fig. 12 provides a schematic diagram of the testing apparatus, the testing device mainly included a servo motor, a CRV-80E reducer, an external load, a swing arm, a high-precision displacement sensor, and a support frame. In testing, the reducer was fixed on the base, which drives the motion's external load to perform reciprocating swing motor. Fig. 13 shows the actual photos of experimental platform and testing apparatus.

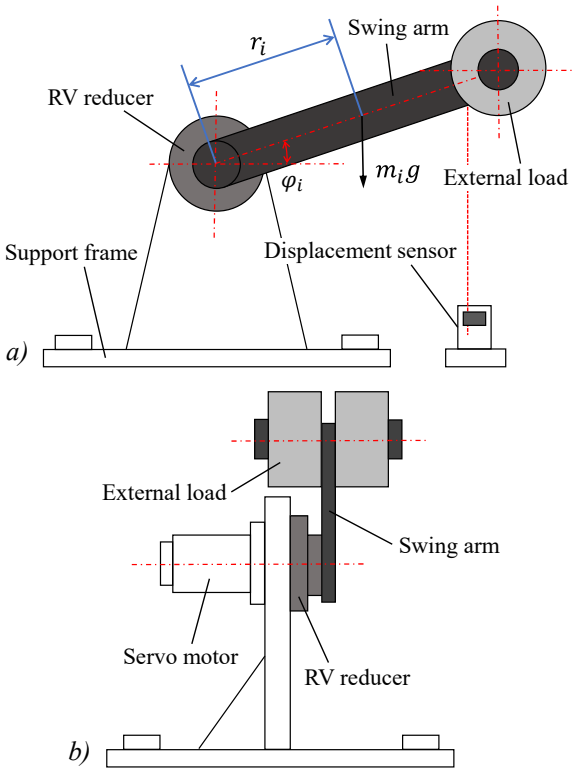

Fig. 12. *Schematic diagram of testing apparatus; a) front view, and b) left view*

The constant stress was adopted for testing, and the accelerated factors were selected as rotating speed or torque. For rotating speed, the high rotation may cause a significant temperature increase for the whole mechanism, resulting in an undeniable impact on output results. Moreover, according to Eq. (15), the effect of torque on accelerated coefficient is greater than rotating speed. Therefore, the torque parameter was selected as the factor to perform the accelerated life test of the reducer. The testbed is installed horizontally with the central axis of the reducer, the load torque of Eq. (24) is given below.

$$T = Qa + \sum\left(m_i g r_i \cos\varphi_i\right). \tag{24}$$

where a is angular acceleration, g is gravitational acceleration, m_i is a mass on a particle, r_i is radius from the particle to central axis, φ_i is rotation angle of the external load centroid on the shaft.

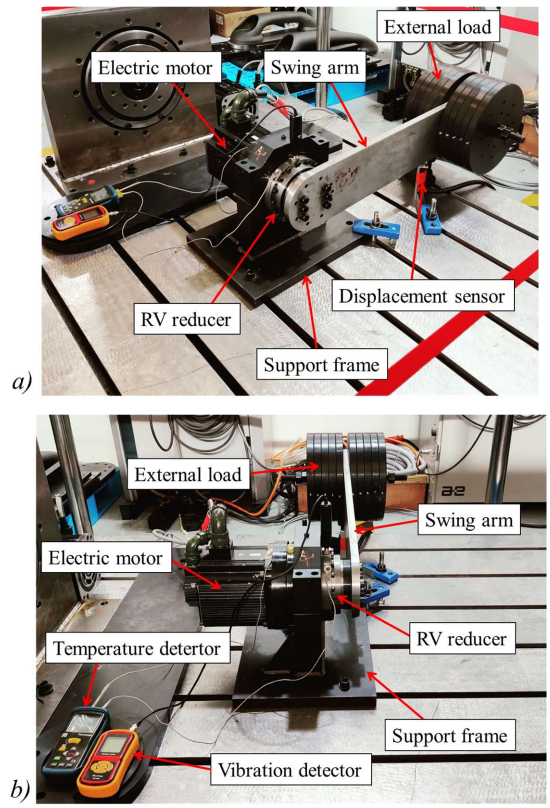

Fig. 13. *Experimental platform and testing apparatus; a) overall view, and b) left view*

3.2 Loading Methods

The swing arm adopted a reciprocating swing loading form, with the rotation angle from 0 to π for one period. It contains the motion stages of static, acceleration, uniform, and deceleration.

In frequent acceleration and deceleration processes, adjusting set parameters can improve its impacts on the reducer. The S-curve is a currently popular algorithm for motion control. The complete S-curve includes the following stages: accelerated acceleration, uniform acceleration, decelerated acceleration, uniform speed, accelerated deceleration, uniform deceleration, and decelerated deceleration [29] and [30]. The following relationships are defined for stage of accelerated acceleration in Eq. (25), where ω is angular speed, t is time.

$$\left.\begin{aligned} j &= \pm j_{\text{const}} \\ a &= jt \\ \omega &= \omega_0 + \frac{1}{2} jt^2 \\ \varphi &= \int_{t_1}^{t_1} \omega dt \end{aligned}\right\}. \tag{25}$$

In testing, the accelerated time of the servo motor is constrained by an external load. The basic parameters for each stage are as follows: an accelerated period of 300 ms, a rated output speed of 15 rpm, an accelerated acceleration period of 100 ms, and a decelerated acceleration period of 100 ms. Moreover, the static state was set to 1000 ms for data collection by a high-precision displacement sensor. The S-curve for acceleration stage and one complete period were obtained based on Eq. (25), as shown in Fig. 14. The figure illustrates a limited value in acceleration, which diminished the impact of the motor on the reducer when loading, and the testing is more in line with the actual working condition.

After determining the mass of the swing arm, the parameters such as torque and average rotating speed at each stage can be calculated by Eqs. (24) and (25), as listed in Table 1. Table 1 shows that the effective load of the RV reducer reached a maximum under the acceleration period with a value of $\Sigma m_i g r_i \cos\varphi_i + 5\pi Q/3$.

3.3 Testing Methods

Based on the above experimental platform, the corresponding accelerated life test was operated with CRV-80E reducer as an testing sample, as shown in Figs. 12 and 13. The input parameters are as follows: $T_0 = 784$ N·m, $n = 15$ rpm, $L_0 = 6000$ h, and the allowable torque for starting and breaking $T_{s1} = 1960$ N·m, instantaneous maximum allowable torque $T_{s2} = 3920$ N·m, and $r = 850$ mm. During testing, it should be ensured that the maximum rotating speed is lower than the rated speed. Set the acceleration torque to 2.5 times of rated value. In this way, the theoretical accelerated lifetime is calculated as $L_a = 290.6$ h, and the accelerated coefficient $A = 20.7$.

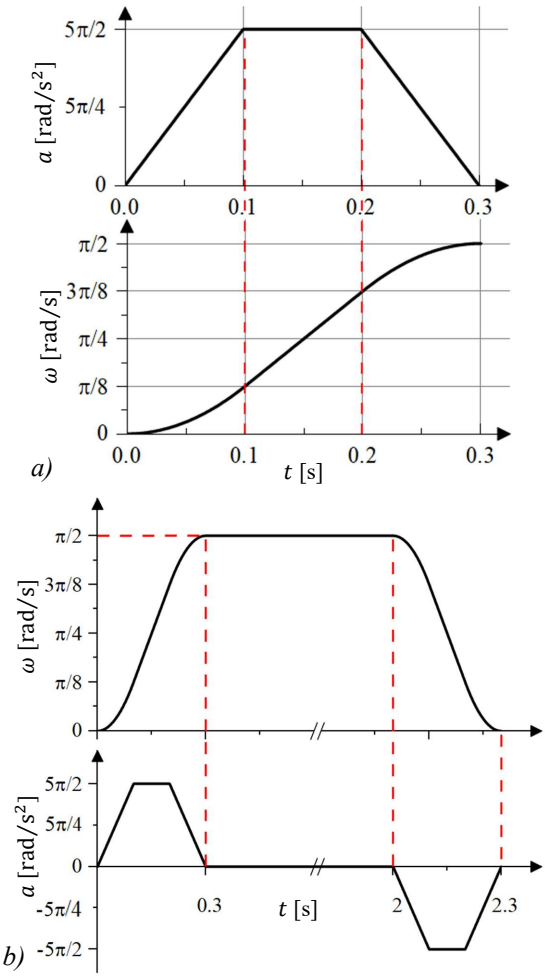

Fig. 14. *S-curve during loading; a) at the acceleration stage, and b) for a single period*

After setting the initial parameters and opening the servo motor, the accelerated life test was performed after the testing apparatus ran stable, with sensors and the acquisition module operating normally. The positioning information of the swing arm was automatically recorded and stored through the displacement sensor. During this period, ensure that the operating environment temperature of the

Table 1. *Experimental parameters under various loading periods*

Periods	Δt [s]	$\Delta\omega$ [rad/s]	$\Delta\varphi$ [rad]	avg a [rad/s^2]	T [N·m]	J [N·m]
Accelerated	0.3	$\pi/2$	$3\pi/40$	$5\pi/3$	$\Sigma m_i g r_i \cos\varphi_i$	$5\pi Q/3$
Uniform	1.7	0	$17\pi/20$	0	$\Sigma m_i g r_i \cos\varphi_i$	$Q\omega^2 l$
Decelerated	0.3	$\pi/2$	$3\pi/40$	$-5\pi/3$	$\Sigma m_i g r_i \cos\varphi_i$	$5\pi Q/3$
Static	1	0	0	0	$m_i g r_i$	0

equipment is consistent with the actual working conditions of the swing arm. The displacement sensor recorded the distance between the detecting probe and the monitoring point on the swing arm. The multiple detection results can be plotted into a point-line diagram, i.e., repeated positioning precision. The test is finished when the value of positioning precision exceeds the allowable range. In other words, the fatigue failure is occurs on the RV reducer at this moment.

3.4 Testing Results and Discussion

Fig. 14 provides the two experimental results for the accelerated test on CRV-80E reducer around 480 hours. Taking the first testing result as an example (Fig. 15a), it depicts that the positioning precision of the RV reducer was stable within the testing time interval of [0,220]. The fitting curve (red dashed line) is distributed relatively flat, i.e., a reducer with high repeated positioning precision. The distance between the highest and lowest points was about 0.1 mm, with a precision loss of 0.02 mm. This stage presented the prime working period of the reducer; after 220 hours, the repeated positioning precision of the reducer sharply decreased; when it reached 270 hours, the positioning precision error reached 0.05 mm, which exceeds the allowable error range for actual application, which indicates that the inside components of reducer may be approaching fatigue failure; after 350 hours testing, the repeated positioning precision sharply decreased with a loss value of 0.16 mm approximately. The error was eight times larger than the prime working period error. Moreover no regression trend proved that the RV reducer no longer met the high-precision requirements after 350 hours of operation, and fatigue failure occurred. For the second testing result (Fig. 15b), the prime working period is in the range of [0,240], and the fatigue failure occurred around 280 hours. In a word, for twice accelerated tests, the accelerated life of the RV reducer is about 270 hours and 280 hours, with 7.09 % and 3.65 % errors compared to the theoretical value of L_a=290.6 h, respectively.

After experiment, the tested RV reducers were disassembled and inspected. It was observed that the inside parts such as involute and cycloidal gears were still under the positive operational conditions. However, the phenomenon of metal peeling fatigue occurred on surface of crankshaft bearing, as shown

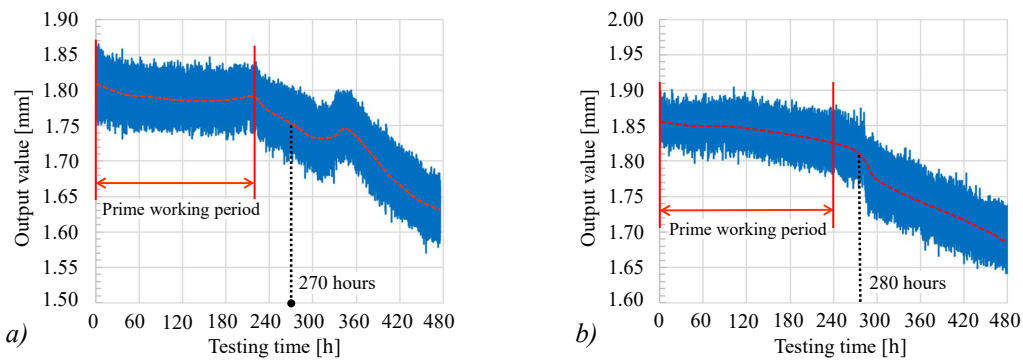

Fig. 15. *Experimental results for accelerated lifespan test of RV reducer; a) first test, and b) second test*

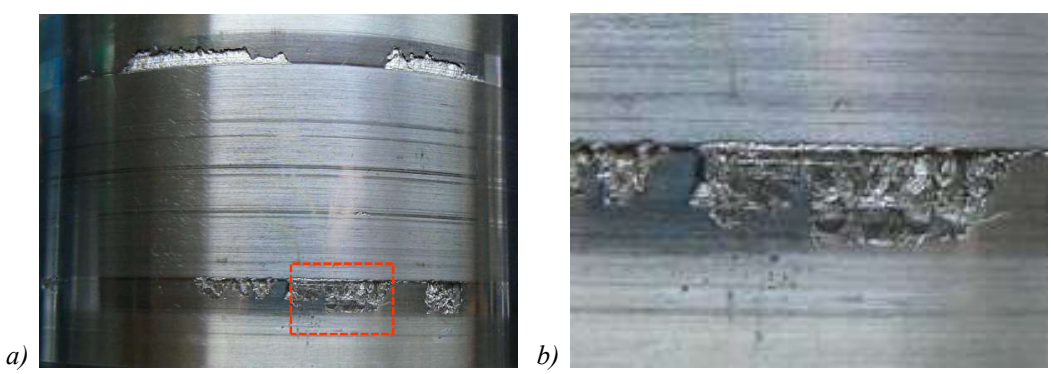

Fig. 16. *Metal peeling failure of RV reducer; a) crankshaft bearing, and b) enlarged part*

in Fig. 16. The results reported the crankshaft bearing was demonstrated as a weak component. Its lifespan has a significant impact on the overall lifespan of RV reducer.

4 CONCLUSIONS

In this study, the CRV-80E reducer is taken as the research object to evaluate its lifespan and reducer test costs. Firstly, the mechanism structure and transmission characteristics were analyzed, with the crankshaft bearing as the key component determining the lifespan of the RV reducer. Based on the fatigue strength theory and Palmgren-Miner linear cumulative damage law, and the theoretical model of fatigue life evaluation for RV reducer was established by analyzing the relationship between fatigue life and torque under various external loads of crankshaft bearing. Secondly, the simulation analysis for contact stress and contact deformation of pin rollers of crankshaft bearings was carried out through ANSYS Workbench and SKF SimPro, respectively. Then, the simulation solutions were compared with the theoretical results from the proposed model. Finally, a testing method for the fatigue life of reducer considering variable external loads was proposed, and the corresponding accelerated life test was designed based on the S-curve control algorithm. The testing results verified the accuracy and feasibility of the theoretical model and simulation solutions. This study can provide a new research method for researchers and reducer manufacturers, and a reference for designers to improve the lifespan of RV reducers by optimizing structural parameters of crankshaft bearing. The conclusions of this study are as follows.

1. The evaluation model of the RV reducer established the relationship between fatigue life and torque under various loads, which can be applied to various components inside the RV reducer with variable external loads. After calculation, the rated life for the CRV-80E reducer is 6008 hours.
2. Comparing the simulation solutions from ANSYS Workbench and SKF SimPro, the errors of contact stress and deformation on rollers of crankshaft bearing are 5.2 % and 6.9 %, respectively, which showed good agreement.
3. The experimental results for the two accelerated life tests were around 270 hours and 280 hours, which was 7.09 % and 3.65 % error compared with the theoretical result, which verified the correctness of fatigue life model. Moreover, the effect of accelerated life on testing is significant. The testing period can be largely diminished.
4. After testing, the reducer was disassembled inspection. It was observed that crankshaft bearing was the first damaged part among all components, which can demonstrate that the crankshaft bearing is the key factor for determining lifespan of the RV reducer.

In future work, one of the potential research topics is exploring the influence of structural parameters of crankshaft bearing, such as the bearing inner diameter, roller radius, and number of rollers, on the lifespan of RV reducer. Reasonably designing the mechanism structure of the crankshaft bearing, the optimal combination of various structural parameters can be researched and solved based on computing algorithms to maximize the fatigue life of the reducer.

5 ACKNOWLEDGEMENTS

This work is supported by the National Key R&D Program of China (Grant No. 2023YFB4704200); National Natural Science Foundation of China (Grant No. 51905009); Key R&D Projects in Hebei Province of China (Grant No. 20311802D).

6 REFERENCES

[1] JIS B0149:1990. *Glossary of Terms and Definitions of Engine*. Japanese Industrial Standards. Tokio.

[2] Bhandri, V.B. (2010). *Design of Machine Elements*. Tata McGraw-Hill Education, New Delhi.

[3] Pham, A.D., Ahn, H.J. (2018). High precision reducers for industrial robots driving 4th Industrial revolution: state of arts, analysis, design, performance evaluation and perspective. *International Journal of Precision Engineering and Manufacturing-Green Technology*, vol. 5, p. 519-533, **DOI:10.1007/s40684-018-0058-x**.

[4] Hsieh, C.F., Feuntez-Aznar., A. (2019). Performance prediction method of cycloidal speed reducers. *Journal of the Brazilian Society of Mechanical Sciences and Engineering*, vol. 41, 186, **DOI:10.1007/s40430-019-1690-2**.

[5] Song, L., Shunke, L., Zheng, Z., Chen, F. (2019). Analysis of the key structures of RV reducer based on finite element method. *IOP Conference Series: Materials Science and Engineering*, vol. 544, no. 1, **DOI:10.1088/1757-899X/544/1/012005**.

[6] Blagojevic, M., Marjanovic, N., Djordjevic, Z., Stojanovic, B., Marjanovic, V., Vujanac, R., Disic, A. (2014). Numerical and experimental analysis of the cycloid disc stress stare. *Tehnicki vjesnik - Tecnical Gazette*, vol. 21, no. 2, p. 377-382.

[7] Zhao, Z., Ye, G., Liu, Y., Zhang, Z. (2021). Recognition of fault state of RV reducer based on self-organizing feature map neural network. *Journal of Physics: Conference Series*, vol. 1986, 012086, **DOI:10.1088/1742-6596/1986/1/012086**.

[8] Zhi, H., Shang, Y. (2020). Remote performance evaluation, life prediction and fault diagnosis of RV reducer for industrial robot. *Journal of Physics: Conference Series*, vol. 1676, 012212, **DOI:10.1088/1742-6596/1676/1/012212**.

[9] Li, X., Shao, W., Tang, J., Ding, H., Zhou, W. (2022). An investigation of the contact fatigue characteristics of an RV reducer crankshaft, considering the hardness gradients and initial residual stress. *Materials*, vol. 15, no. 21, 7850, **DOI:10.3390/ma15217850**.

[10] Gao, S., Zhang, Y., Ji, S., Li, Y., Li, W. (2024). Multi-objective optimized design for modified cycloid-pin gear drive mechanism based on load-bearing capacity. *Journal of Advanced Mechanical Design, Systems, and Manufacturing*, vol. 18, no. 2, **DOI:10.1299/jamdsm.2024jamdsm0015**.

[11] Zhao, Y., Han, Z., Tan, Q., Shan, W., Li, R., Wang, H., Du, Y. (2024). Multi-Objective Optimization Design of Cycloid-Pin Gears Based on RV Reducer Precision Transmission Performance. *Energies*, vol. 17, no. 3, 654, **DOI:10.3390/en17030654**.

[12] Huang, J., Li, C., Chen, B. (2020). Optimization design of RV reducer crankshaft bearing. *Applied Sciences*, vol. 10, no. 18, 6520, **DOI:10.3390/app10186520**.

[13] Nentwich, C., Reinhart, G. (2021). A method for health indicator evaluation for condition monitoring of industrial robot gears. *Robotics*, vol. 10, no. 2, 80, **DOI:10.3390/robotics10020080**.

[14] Lee, G., Kim, H., Kim, D. (2003). Study of the accelerated life test method for power train components under cyclic loads using Weibull-IPL (inverse power law) model. *ASME International Mechanical Engineering Congress and Exposition*, vol. 37122, p. 535-541, **DOI:10.1115/IMECE2003-42652**.

[15] Wang, W., Durack, J. M., Durack, M. J., Zhang, J., Zhao, P. (2021). Automotive traction drive speed reducer efficiency testing. *Automotive Innovation*, vol. 4, p. 81-92, **DOI:10.1007/s42154-021-00135-3**.

[16] Wang, Y., Wei, B., Wang, Z., Yang, J., Xu, J. (2023). Research on loaded contact analysis and tooth wear calculation method of cycloid-pin gear reducer. *Lubricants*, vol. 11, no. 10, 445, **DOI:10.3390/lubricants11100445**.

[17] Yang, M., Zhang, D., Cheng, C., Han, X. (2021). Reliability-based design optimization for RV reducer with experimental constraint. *Structure and Multidisciplinary Optimization*, vol. 63, p. 2047-2064, **DOI:10.1007/s00158-020-02781-3**.

[18] Krockenberger, O. (1996). Industrial robots for the automotive industry. *Sae Brasil 96 V International Mobility Technology Conference & Exhibit*, vol. 1, **DOI:10.4271/962393**.

[19] Litvin, F.L., Feng, P.H. (1996). Computerized design and generation of cycloidal gearings. *Mechanism and Machine Theory*, vol. 31, no. 7, p. 891-911, **DOI:10.1016/0094-114X(95)00115-F**.

[20] Qian, H., Li, Y., Huang, H. (2020). Time-variant reliability analysis for industrial robot RV reducer under multiple failure modes using Kriging model. *Reliability Engineering & System Safety*, vol.199, 106936, **DOI:10.1016/j.ress.2020.106936**.

[21] Hashin, Z., Rotem, A. (1978). A cumulative damage theory of fatigue failure. *Materials Science and Engineering*, vol. 34, no. 2, p. 147-160, **DOI:10.1016/0025-5416(78)90045-9**.

[22] Brown, M.W., Miller, K.J. (1973). A theory for fatigue failure under multiaxial stress-strain conditions. *Proceedings of the institution of Mechanical Engineers*, vol. 187, no. 1, p. 745-755, **DOI:10.1243/PIME_PROC_1973_187_161_02**.

[23] Miller, K.J., Zachariah, K.P. (1977). Cumulative damage laws for fatigue crank initiation and stage 1 propagation. *The Journal of Strain Analysis for Engineering Design*, vol. 12, no. 4, p. 262-270, **DOI:10.1243/03093247V124262**.

[24] Harris, T.A., Kotzalas, M.N. (2006). *Rolling Bearing Analysis,* Taylor & Francis Group, CRC Press.

[25] Vencl, A., Rac, A. (2014). Diesel engine crankshaft journal bearings failures: case study. *Engineering Failure Analysis*, vol. 44, p. 217-228, **DOI:10.1016/j.engfailanal.2014.05.014**.

[26] Litvin, F.L., Fuentes, A. (2004). *Gear Geometry and Applied Theory*. Cambridge University Press, Cambridge, **DOI:10.1017/CBO9780511547126**.

[27] ISO 281:2007. *Rolling Bearings - Dynamic Load Ratings and Rating Life*. International Standard Organization. Geneva.

[28] Machado, M., Moreira, P., Flores, P., Lankarani, H.M. (2012). Compliant contact force models in multibody dynamics: Evolution of the Hertz contact theory. *Mechanism and Machine Theory*, vol. 53, p. 99-121, **DOI:10.1016/j.mechmachtheory.2012.02.010**.

[29] Lu, J.W., Beamish, P.W. (2004). International diversification and firm performance: The S-curve hypothesis. *Academy of Management Journal*, vol. 47, no. 4, p. 598-609, **DOI:10.5465/20159604**.

[30] Shaji, E., Vemugopal, P.R., Velayudhan, G., Selvakumar, M. (2022). Fatigue life prediction of butt weld joint with weld defects at multiple locations. *Strojniški vestnik - Journal of Mechanical Engineering*, vol. 68, no. 5, p. 350-358, **DOI:10.5545/sv-jme.2021.7536**.